Axial Ligand Orientation in Iron(III) Porphyrinates: Effect of Axial .pi.-Acceptors. Characterization of the Low-Spin Complex [Fe(TPP)(4-CNPy)2]ClO4

7 AUTHORS, INCLUDING:

F(rances) Ann Walker
The University of Arizona
240 PUBLICATIONS **8,646** CITATIONS

SEE PROFILE

Arnold M Raitsimring
The University of Arizona
123 PUBLICATIONS **2,578** CITATIONS

SEE PROFILE

W. Patrick Walters
Vertex Pharmaceuticals
38 PUBLICATIONS **2,678** CITATIONS

SEE PROFILE

W. Robert Scheidt
University of Notre Dame
363 PUBLICATIONS **13,272** CITATIONS

SEE PROFILE

Axial Ligand Orientation in Iron(III) Porphyrinates: Effect of Axial π-Acceptors. Characterization of the Low-Spin Complex [Fe(TPP)(4-CNPy)₂]ClO₄

Martin K. Safo,[1a] F. Ann Walker,*[,1b] Arnold M. Raitsimring,[1b] W. Patrick Walters,[1b] Daniel P. Dolata,[1b] Peter G. Debrunner,*[,1c] and W. Robert Scheidt*[,1a]

Contribution from the Department of Chemistry and Biochemistry, University of Notre Dame, Notre Dame, Indiana 46556, Department of Chemistry, University of Arizona, Tucson, Arizona 85721, and Department of Physics, University of Illinois, Urbana, Illinois 61801

Received March 1, 1994[®]

Abstract: The preparation and characterization of the low-spin bis(pyridine)iron(III) porphyrinate complex [Fe(TPP)-(4-CNPy)₂]ClO₄ is reported. Consistent with the expected effect from the strong π-acceptor character of the axial 4-cyanopyridine ligands, the X-ray structure of the complex shows that the two axial ligands have relative perpendicular orientations along with an extensively S_4-ruffled porphyrin core. The S_4 ruffling is among the largest found for bis(pyridine) complexes and leads to the extremely short average Fe–N_P bond distance of 1.952(7) Å. The axial Fe–N bond distances average to 2.002(8) Å. Molecular mechanics calculations indicate that the ruffling observed in this and other bis(pyridine) complexes of Fe(III) porphyrins is not simply a result of steric interactions between the phenyl rings and the pyridine ligands, since the minimized energies of bis(pyridine) complexes of the non-phenyl-containing system, [Fe(porphine)(pyridine)₂]⁺, as a function of the angular orientation of two perpendicularly aligned pyridine ligands with respect to the N–Fe–N axes of the porphyrin ring, are within experimental error of those of [Fe(TPP)-(pyridine)₂]⁺. Therefore, the observed strong S_4 ruffling of the porphyrinato core must be due to electronic rather than steric factors. This electronic contribution is likely the partial delocalization of the d_{xy} unpaired electron into the $a_{2u}(\pi)$ orbital of the porphyrin ring, which is made possible by the twisting of the nitrogen p_z orbitals out of the mean plane of the porphyrin ring as a result of the strong S_4 ruffling. The Mössbauer spectrum of the complex has an isomer shift of 0.19(1) mm/s and an unusually small quadrupole splitting (ΔE_q) of 0.65(1) mm/s. The EPR spectra in both solid and solution phases are axial, with $g_\perp \geq 2.62$ and $g_\parallel \leq 0.92$ at 4.2 K, $\Sigma g^2 \sim 14.6$. The [Fe(TPP)(4-CNPy)₂]ClO₄ complex is thus a case in which a large amount of the d orbital angular momentum of the metal is quenched, and hence Σg^2 is much lower than 16, and is, in fact, midway between that value and the minimum possible value of 12 that is expected for a pure $(d_{xy})^1$ unpaired electron. Single crystal EPR spectra show a strong broadening of the EPR signal near the $g_\parallel$ turning point that is indicative of what has been called by some researchers "g-strain," as was previously observed in the "large g_{max}" type of rhombic EPR signals of low-spin Fe(III) porphyrin systems having perpendicularly aligned planar axial ligands and a $(d_{xy})^2(d_{xz},d_{yz})^3$ electronic ground state (Walker, F. A.; Huynh, B. H.; Scheidt, W. R.; Osvath, S. R. *J. Am. Chem. Soc.* **1986,** *108,* 5288–5297). The inability to observe the minimum g-value in this axial system is a result of the strong dependence of $g_\parallel$ on the field strength of the ligands, as measured by the tetragonality (Δ/λ). All physical properties are consistent with an iron(III) ion that has the unusual ground-state configuration $(d_{xy},d_{yz})^4(d_{xy})^1$. Crystal data for [Fe(TPP)(4-CNPy)₂]ClO₄·CH₂Cl₂: $a = 11.187(11)$ Å, $b = 20.208(11)$ Å, $c = 21.815(18)$ Å, orthorhombic, space group $P2_12_12_1$, $V = 4931.5$ Å³, $Z = 4$, no. obsd data = 5662.

Introduction

There have been a number of recent investigations of the relative orientations of planar axial ligands in Fe(III) porphyrinates.[2–10] Among the cytochromes of known molecular structures that are involved in electron transfer (cytochromes b_4[11] and c_3[12]), two types of limiting structures and two types of EPR spectra have been observed. Cytochrome b_5 and three of the four hemes of cytochromes c_3 have the imidazole rings of the two coordinated

histidines in nearly parallel planes, while one heme in the cytochromes c_3 of known structures has its imidazole rings in nearly perpendicular planes.[12] The EPR spectra of cytochromes b_5[13–15] and three of the hemes of the cytochromes c_3[16] are rhombic, with $g_{zz} \sim 2.9$–3.0, $g_{yy} \sim 2.25$–2.35, and $g_{xx} \sim 1.4$–1.6, typical of the class of heme proteins called "B hemichromes" by Blumberg and Peisach.[17] The fourth heme has a single feature EPR signal at $g = 3.3$–3.7[16] that we have called the "strong g_{max}"[18] or "large g_{max}"[2] signal. In addition, there are a number of membrane-bound cytochromes b with probable bis(histidine) coordination,[19] including the two cytochromes b of mitochondrial "complex III" (also known as ubiquinone–cytochrome c oxidoreductase) as well as chloroplast cytochrome b_6. These have large g_{max} EPR spectra[20] and a wider range of reduction potentials than observed for the cytochromes b_5 and b_2, and the b heme of sulfite oxidase, all of

® Abstract published in *Advance ACS Abstracts,* July 15, 1994.

(1) (a) University of Notre Dame. (b) University of Arizona. (c) University of Illinois.

(2) Walker, F. A.; Huynh, B. H.; Scheidt, W. R.; Osvath, S. R. *J. Am. Chem. Soc.* **1986,** *108,* 5288.

(3) Scheidt, W. R.; Kirner, J. L.; Hoard, J. L.; Reed, C. A. *J. Am. Chem. Soc.* **1987,** *109,* 1963.

(4) Hatano, K.; Safo, M. K.; Walker, F. A.; Scheidt, W. R. *Inorg. Chem.* **1991,** *30,* 1643.

(5) Safo, M. K.; Gupta, G. P.; Walker, F. A.; Scheidt, W. R. *J. Am. Chem. Soc.* **1991,** *113,* 5497.

(6) Safo, M. K.; Gupta, G. P.; Watson, C. T.; Simonis, U.; Walker, F. A.; Scheidt, W. R. *J. Am. Chem. Soc.* **1992,** *114,* 7066.

(7) Scheidt, W. R.; Chipman, D. M. *J. Am. Chem. Soc.* **1986,** *108,* 1163.

(8) Quinn, R.; Valentine, J. S.; Byrn, M. P.; Strouse, C. E. *J. Am. Chem. Soc.* **1987,** *109,* 3301.

(9) Soltis, S. M.; Strouse, C. E. *J. Am. Chem. Soc.* **1988,** *110,* 2824.

(10) Inniss, D.; Soltis, S. M.; Strouse, C. E. *J. Am. Chem. Soc.* **1988,** *110,* 5644.

(11) Mathews, F. S.; Czerwinski, E. W.; Argos, P. In *The Porphyrins;* Dolphin, D., Ed.; Academic Press: New York, 1979; Vol. VII, p 108.

(12) Pierrot, M.; Haser, R.; Frey, M.; Payan, F.; Astier, J.-P. *J. Biol. Chem.* **1982,** *257,* 14341. Higuchi, Y.; Kusunoki, M.; Matsuura, Y.; Yasuoka, N.; Kakudo, M. *J. Mol. Biol.* **1984,** *172,* 109.

(13) Bois-Poltoratsky, R.; Ehrenberg, A. *Eur. J. Biochem.* **1967,** *2,* 361.

(14) Passon, P. G.; Reed, D. W.; Hultquist, D. E. *Biochim. Biophys. Acta* **1972,** *275,* 51.

(15) Rivera, M.; Barillas-Mury, C.; Christensen, K. A.; Little, J. W.; Wells, M. A.; Walker, F. A. *Biochemistry* **1992,** *31,* 12233.

which have rhombic, typical B hemichrome EPR spectra. There is thus the possibility of a correlation between the axial ligand plane orientation and the reduction potential.[21,22]

Investigation of the molecular structures, EPR spectra, and in some cases Mössbauer spectra of well-defined low-spin heme model compounds has provided conclusive proof that the large g_{max} EPR signal is correlated with near-axial symmetry[2,10] and, for planar axial ligands, with perpendicular alignment of these ligands.[2,4,5] The first investigation of this type[2] was of $[Fe(TPP)(ImH)_2]^+Cl^-$,[23,24] which has the axial ligands in parallel planes and two overlapping rhombic EPR signals consistent with two different projections of the parallel imidazole planes on the porphinato core. On the other hand, $[Fe(TPP)(2\text{-MeImH})_2]^+$-$ClO_4^-$ [3] has the axial ligands in perpendicular planes and a large g_{max} feature at $g = 3.41$.[2] Mössbauer spectra at 4.2 K in a small applied magnetic field (500 G) allowed estimation of the two unresolved g-values.[2]

Griffith's theory[25] and Taylor's formulation[26] were used to calculate relative energies of the d_{xy}, d_{xz}, and d_{yz} orbitals for the two complexes and the idealized parallel and perpendicular orientations of the axial imidazoles.[2] The results confirm that the parallel orientation is more stable and that perpendicular alignment of planar axial ligands could lead to a positive shift in reduction potential of up to ~50 mV over that observed for parallel alignment, all other structural and environmental factors being equal.[2] Strouse and co-workers then showed that for parallel alignment of imidazoles bound to low-spin Fe(III) porphyrins, a "pseudo-Jahn–Teller" distortion of the porphyrin ligand can contribute significantly to the rhombic splitting.[8,9] They also found that while crystal field stabilization of the parallel orientation is significant for strong π-donor axial ligands such as imidazoles, for weak π-donors, such as pyridine, and for nonplanar ligands, such as cyanide, spin–orbit stabilization results in near degeneracy of the d_{xz} and d_{yz} orbitals.[10] This again suggests the possibility of real differences in reduction potentials of low-spin porphinatoiron(III) complexes having parallel *vs* perpendicular axial ligand planes. More recent findings include the fact that even strong π-donor pyridine ligands, such as 4-(dimethylamino)-pyridine, can be forced to bind with perpendicular planes if bulky groups are placed at the periphery of the porphyrin, as in Fe^{III}-(TMP) derivatives, and, again, a large g_{max} EPR signal is observed ($g = 3.48$).[5]

Our recent determinations of the structures of a series of $[Fe(TMP)(L)_2]ClO_4$ complexes in which L is a pyridine (4-NMe_2-Py,[5] 3-EtPy,[6] 3-ClPy,[6] 4-CNPy,[6] and 3-CNPy[6]) or hindered imidazole[27] show that, as expected from their large g_{max} EPR spectra,[5,6] both pyridine and hindered imidazole ligands are aligned

in perpendicular planes. The nonbonded interactions between the ortho H of the pyridine ligands or the 2-CH_3 of the hindered imidazole ligands and the methyl groups of the porphyrin mesityl rings produce a strongly ruffled porphyrin core having two oblong "cavities" at right angles to each other, one above and one below the plane of the porphyrin, which hold the axial ligands in perpendicular planes over the meso positions. In the complexes of low-basicity pyridines, we noted both large variations and unusually low EPR g-values and Mössbauer quadrupole splittings.[6] We suggested that the large range and especially the unusually small ΔE_q and g-values were related to the axial ligand π-bonding properties, which led to significant changes in the relative energies of the d_{xy}, d_{xz}, and d_{yz} orbitals.[6] Indeed, with very strong π-accepting ligands, such as 3- and 4-cyanopyridines, the orbital energies appear to have changed so markedly that the d_{xy} orbital is *higher* in energy than the d_{xz}, d_{yz} pair.[6] In other words, there are two quite distinct, limiting ground states for low-spin iron(III) in this series of iron(III) porphyrinates: (a) the generally observed $(d_{xy})^2(d_{xz},d_{yz})^3$ state or (b) the novel $(d_{xz},d_{yz})^4(d_{xy})^1$ state where the d_{xz},d_{yz} pair is degenerate, or nearly so, and *below* the d_{xy} orbital in energy. This latter electronic state leads to an *axial* EPR spectrum, with $g_\perp > g_\parallel$,[6] rather than the usual rhombic or large g_{max} EPR signal.[2,5] The unusual EPR and Mössbauer parameters of these low-basicity pyridine complexes were fully reflected in their ¹H NMR spectra; at –80 °C, the pyrrole-H isotropic shifts varied smoothly from –40 ppm (L = 4-NMe_2Py) to –6 ppm (L = 4-CNPy) as the basicity of the pyridine ligand decreased.[6] Earlier ¹H NMR investigations of the related $[Fe(TPP)(L)_2]^+$ complexes by La Mar and co-workers[28] had shown a similar but less pronounced trend in the pyrrole-H isotropic shifts as a function of pyridine basicity.

Based on both EPR and NMR spectroscopic data, it has been accepted that low-spin Fe(III) porphyrinates have a $(d_{xy})^2(d_{xz},d_{yz})^3$ ground state.[29,30] This ground state gives rise to rhombic EPR spectra and ¹H NMR spin delocalization to protons on the periphery of the molecule *via* the filled 3e(π) porphyrin orbitals, *i.e.*, P → Fe π-bonding.[29,30] Recent 2-D NMR (COSY) studies of unsymmetrically phenyl-substituted derivatives of $[Fe(TPP)$-$(N\text{-MeIm})_2]^+$ conclusively show that the pattern of spin delocalization to the β-pyrrole positions is exactly that expected for the 3e(π) orbitals, as modified by the electron-donating or -withdrawing characteristics of the substituent.[31] However, it has also recently been shown[6,32,33] that with certain kinds of axial ligands (isonitriles,[33,34] low-basicity pyridines[6,28]) or certain modifications of the porphyrin π orbitals (such as occurs in the reduced hemes), the relative energies of the d_{xy} and d_π orbitals (d_{xz},d_{yz}) can be reversed, leading to a $(d_{xz},d_{yz})^4(d_{xy})^1$ electron configuration. This electron configuration results in axial (with $g_\perp > 2 > g_\parallel$)[6,30] or near-axial EPR spectra,[35] and, in some cases, ¹H NMR spectra that show just the reverse types of π spin delocalization patterns: negligible π spin delocalization to the β-pyrrole positions but large π spin delocalization to the meso positions.[6,30] However, the d_{xz},d_{yz} orbital set, which has proper symmetry for π spin delocalization, is filled, and the d_{xy} orbital does not have proper symmetry for overlap with any of the π

(16) Cammack, R.; Fauque, D.; Moura, J. J. G.; LeGall, J. *Biochim. Biophys. Acta* **1984**, *784*, 68. Gayda, J. P.; Bertrand, P.; More, C.; Guerlesquin, F.; Bruschi, M. *Biochim. Biophys. Acta* **1985**, *829*, 262. Gayda, J. P.; Yagi, T.; Bensman, H.; Bertrand, P. *FEBS Lett.* **1987**, *217*, 57. Gayda, J. P.; Benosman, H.; Bertrand, P.; More, C.; Asso, M. *Eur. J. Biochem.* **1988**, *177*, 199. Moura, I.; Teixeira, M.; Huynh, B. H.; LeGall, J.; Moura, J. J. *Eur. J. Biochem.* **1988**, *176*, 365.

(17) Blumberg, W. E.; Peisach, J. *Adv. Chem. Ser.* **1971**, *100*, 271.

(18) Walker, F. A.; Reis, D.; Balke, V. L. *J. Am. Chem. Soc.* **1984**, *106*, 6888.

(19) Widger, W. R.; Cramer, W. A.; Herrmann, R. G.; Trebst, A. *Proc. Natl. Acad. Sci. U.S.A.* **1984**, *81*, 674. Babcock, G. T.; Widger, W. R.; Cramer, W. A.; Oertling, W. A.; Metz, J. *Biochemistry* **1985**, *24*, 3638.

(20) Carter, K. R.; Tsai, A.-L.; Palmer, G. *FEBS Lett.* **1981**, *132*, 243. Salerno, J. C. *J. Biol. Chem.* **1984**, *259*, 2331. Bergström, J. *FEBS Lett.* **1985**, *183*, 87.

(21) For example, the reduction potentials of the four hemes of cytochromes c_3 vary over a range of ~200–300 mV.[16,22]

(22) Niki, K.; Kawasaki, Y.; Nishimura, N.; Higuchi, Y.; Yasuoka, N.; Kakudo, M. *J. Electroanal. Chem.* **1984**, *168*, 275.

(23) Scheidt, W. R.; Osvath, S. R.; Lee, Y. J. *J. Am. Chem. Soc.* **1987**, *109*, 1958.

(24) Abbreviations used include 4-CNPy, 4-cyanopyridine; OEP, dianion of octaethylporphyrin; TPP, dianion of *meso*-tetraphenylporphyrin; TMP, dianion of *meso*-tetramestiylporphyrin; N_P, porphinato nitrogen atom; N_{ax}, axial ligand nitrogen.

(25) Griffith, J. S. *Proc. R. Soc. London, A* **1956**, *235*, 23.

(26) Taylor, C. P. S. *Biochim. Biophys. Acta* **1977**, *491*, 137.

(27) Munro, O. Q.; Marques, H. M.; Debrunner, P. G.; Mohanrao, K.; Scheidt, W. R. Submitted for publication.

(28) La Mar, G. N.; Bold, T. J.; Satterlee, J. D. *Biochim. Biophys. Acta* **1977**, *498*, 189.

(29) La Mar, G. N.; Walker, F. A. In *The Porphyrins*; Dolphin, D., Ed.; Academic Press: New York, 1979; Vol. IVB, pp 57–161.

(30) Walker, F. A.; Simonis, U. In *Biological Magnetic Resonance, Volume 12: NMR of Paramagnetic Molecules*; Berliner, L. J., Reuben, J., Eds.; Plenum Press: New York, 1993; pp 133–274.

(31) Lin, Q.; Simonis, U.; Tipton, A. R.; Norvell, C. J.; Walker, F. A. *Inorg. Chem.* **1992**, *31*, 4216.

(32) Watson, C. T.; Simonis, U.; Walker, F. A., to be submitted.

(33) Nasri, H.; Turowska-Tyrk, I.; Mohanrao, K.; Watson, C. T.; Debrunner, P. G.; Walker, F. A.; Scheidt, W. R., to be submitted.

(34) Simonneaux, G.; Hindre, F.; Le Plouzennec, M. *Inorg. Chem.* **1989**, *28*, 823.

(35) Stolzenberg, A. M.; Strauss, S. H.; Holm, R. H. *J. Am. Chem. Soc.* **1981**, *103*, 4763.

7762 *J. Am. Chem. Soc., Vol. 116, No. 17, 1994*

Safo et al.

orbitals of the porphyrin ring.[36,37] This apparent paradox was first explained in terms of fractional occupation of the d_{xz}, d_{yz} orbital set due to spin–orbit mixing of these orbitals with d_{xy},[6] but more recently it has been shown that the amount of unpaired electron delocalized to the meso substituents is larger than can be explained by the spin–orbit mixing of these orbitals.[30] This point will be discussed further in this work.

The unusual properties of the iron(III) tetramesitylporphyrinate derivatives with 3- or 4-cyanopyridine as axial ligand[6] have led us to examine other iron(III) tetraarylporphyrinate derivatives with 4-cyanopyridine. If the π-accepting character of the 4-cyanopyridine ligand dominates the bonding in low-spin Fe-(III) derivatives, we would expect to find the two axial ligands with relative perpendicular orientations, representing another example of (in limiting terms) the unusual $(d_{xz}, d_{yz})^4(d_{xy})^1$ ground state. In this paper, we present the preparation and characterization of [Fe(TPP)(4-CNPy)$_2$]ClO$_4$. The X-ray crystal structure and the Mössbauer and EPR spectra of [Fe(TPP)(4-CNPy)$_2$]-ClO$_4$ have been determined; all properties are consistent with strong π-accepting properties of the axial ligands, and they suggest an electronic contribution to the observed ruffling of the porphyrin ring.

Experimental Section

General Information. Reactions were performed with solvents distilled under argon prior to use. THF and chlorobenzene were distilled from sodium benzophenone ketyl, and dichloromethane and hexane were distilled from CaH$_2$. 4-Cyanopyridine was recrystallized from CH$_2$Cl$_2$. The [Fe(TPP)(4-CNPy)$_2$]ClO$_4$ complex was prepared by reacting a chlorobenzene–CH$_2$Cl$_2$ solution (10 mL) of [Fe(TPP)(OClO$_3$)] (100 mg, 0.130 mmol) with 4-cyanopyridine (271 mg, 2.60 mmol) under an argon atmosphere. *Caution!* Perchlorate salts are potentially explosive when heated or shocked. Handle them in milligram quantities with care. The reaction mixture was shaken for 1 min, filtered, and then layered with hexane for crystallization. X-ray quality crystals formed after 4 days. UV–vis spectra were recorded on a Perkin-Elmer Lambda 4C spectrophotometer and IR spectra on a Perkin-Elmer 883 spectrophotometer with samples as KBr pellets. Mössbauer samples were prepared by Apiezon L grease mulls; measurements were made at 4.2 and 120 K on a constant acceleration Mössbauer spectrometer. The 120 K spectra were least-squares fitted with Lorentzian or Voigt line shapes.[38] Isomer shifts are quoted relative to iron metal at 300 K. EPR spectra were recorded on a Bruker ESP-300E EPR spectrometer operating at X-band and equipped with an Oxford helium cryostat. Spectra were obtained for samples in frozen CH$_2$Cl$_2$ solution and as polycrystalline and single crystal solids.

Structure Determination. Crystalline [Fe(TPP)(4-CNPy)$_2$]ClO$_4$ was examined on an Enraf-Nonius CAD4 diffractometer equipped with a locally modified Syntex LT-1 low-temperature attachment. Preliminary examination at 118 K led to the assignment of a four-molecule orthorhombic cell, space group $P2_12_12_1$. Final cell constants and complete details of the intensity collection and least-squares refinement parameters are summarized in Tables 1 and SI. Precise cell constants were determined from least-squares refinement of 25 automatically centered reflections. Four standard reflections were monitored during data collection for crystal movements and possible deterioration of the crystal. No significant decay was observed.

Intensity data were reduced using the data reduction suite of R. H. Blessing.[39] All data with $F_o \geq 3.0\sigma(F_o)$ were retained as observed and used in all subsequent refinements. The structure was solved with the direct methods program MULTAN[40] and difference Fourier syntheses. The structure consists of one porphyrin molecule and one CH$_2$Cl$_2$ solvent molecule in the asymmetric unit. Structure solution was straightforward

Table 1. Summary of Crystal Data and Intensity Collection Parameters for [Fe(TPP)(4-CNPy)$_2$]ClO$_4$·CH$_2$Cl$_2$

formula	FeCl$_3$O$_4$N$_8$C$_{57}$H$_{38}$
fw, amu	1061.19
space group	$P2_12_12_1$
T, K	118
a, Å	11.187(11)
b, Å	20.208(11)
c, Å	21.815(18)
V, Å^3	4931.5
Z	4
no. observed data	5662
D(obsd), g/cm^3	1.41[a]
D(calcd), g/cm^3	1.43[a]
R_1	0.058
R_2	0.063

[a] D(obsd) obtained at 294 K, and D(calcd) obtained at 118 K.

except for disorder in the perchlorate anion. Two of the oxygen atoms were disordered over two positions. These positions were assigned occupancies of 0.75 and 0.25 and included in the full-matrix least-squares refinements. After several cycles of least-squares refinement, the probable locations of most hydrogen atoms were found in difference Fourier maps. Hydrogen atom positions were idealized and included in subsequent cycles of least-squares refinement as fixed contributors (C–H = 0.95 Å and B(H) = 1.3B(C)), with additional reidealization as required. All atoms were refined anisotropically except hydrogens and the two disordered oxygen atoms with occupancies of 0.25. The correct enantiomeric form had been originally chosen; refinement of the other enantiomer led to significantly higher values of the discrepancy indices ($\sim$0.8% higher). Final atomic coordinates, final anisotropic temperature factors, hydrogen atom positions, and structure factor tables are listed in Tables SI–SV (supplementary material).

Molecular Mechanics Calculations. All energy minimizations were carried out using the MM2* force field in Macromodel 3.5[41] on a Silicon Graphics Iris Indigo workstation. Additional parameters for the porphyrin system were taken from Munro et al.[42] The parameters added to the standard Macromodel MM2* parameter set are listed in Table SVI (supplementary material). Crystal structures were obtained from version 5.05 of the Cambridge Crystallographic Database. The [Fe(TPP)(Py)$_2$]+ structure was taken from reference code GEWKOI.[10] For comparison, the [Fe(TMP)(4-NMe$_2$Py)$_2$]+ structure from reference code VOFLUX[5] was used. The [Fe(porphine)(Py)$_2$]+ structure was derived from the [Fe(TPP)(Py)$_2$]+ structure by replacement of the phenyl rings with hydrogen atoms at a bond length of 1.01 Å.

Results

[Fe(TPP)(4-CNPy)$_2$]ClO$_4$ has been characterized by an X-ray structure determination and Mossbauer, EPR, IR, and UV–vis spectroscopy. In addition, the conformational preferences and barriers to axial ligand rotation have been investigated by molecular mechanics calculations (MM2*) and visualized by means of the Macromodel program.[41] The molecular structure of [Fe(TPP)(4-CNPy)$_2$]ClO$_4$ is shown in the ORTEP diagram (Figure 1) along with the numbering scheme for the crystallographically unique atoms. [Fe(TPP)(4-CNPy)$_2$]ClO$_4$ has its axial pyridine ligands in relative perpendicular orientation. The projections of the axial ligand planes are close to bisecting adjacent

(36) It must be noted that because the temperatures at which EPR and NMR spectra are recorded, 4–77 K *vs* $\sim$180–340 K, respectively, are so different, there is not necessarily a direct correspondence between the electron configuration observed by EPR spectroscopy and that observed by NMR spectroscopy.[30] This appears to be particularly true of the low-spin Fe(III) complexes of the reduced hemes.[37]

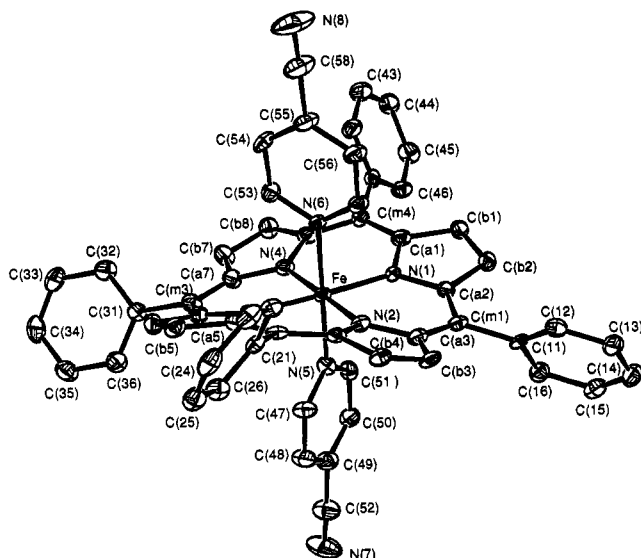(37) Keating, K. A.; La Mar, G. N.; Shiau, F.-Y.; Smith, K. M. *J. Am. Chem. Soc.* **1992**, *114*, 6513.

(38) Chrisman, B. L.; Tumolillo, B. *Comput. Phys. Commun.* **1971**, *2*, 322–330.

(39) Blessing, R. H. *Cryst. Rev.* **1987**, *1*, 3.

(40) Programs used in this study included local modifications of Main, Hull, Lessinger, Germain, Declerq, and Woolfson's MULTAN, Jacobson's ALLS, Zalkin's FORDAP, Busing and Levy's ORFFE, and Johnson's ORTEP2. Atomic form factros were from: Cromer, D. T.; Mann, J. B. *Acta Crystallogr., Sect. A* **1968**, *24*, 321. Real and imaginary corrections for anomalous dispersion in the form factor of the iron atom were from: Cromer, D. T.; Liberman, D. J. *J. Chem. Phys.* **1970**, *53*, 1891. Scattering factors for hydrogen were from: Stewart, R. F.; Davidson, E. R.; Simpson, W. T. *J. Chem. Phys.* **1965**, *42*, 3175. All calculations were performed on a VAXstation 3200 computer.

(41) Mohamadi, F.; Richards, N. G. J.; Guida, W. C.; Liskamp, R.; Lipton, M.; Caufield, C.; Chang, G.; Hendrickson, T.; Still, W. C. *J. Comput. Chem.* **1990**, *11*, 440.

(42) Munro, O. Q.; Bradley, J. C.; Hancock, R. D.; Marques, H. M.; Marsicano, F.; Wade, P. W. *J. Am. Chem. Soc.* **1992**, *114*, 7218.

Axial Ligand Orientation in Iron(III) Porphyrinates

J. Am. Chem. Soc., Vol. 116, No. 17, 1994 7763

Figure 1. ORTEP diagram of [Fe(TPP)(4-CNPy)$_2$]ClO$_4$. Labels assigned to the crystallographically unique atoms are displayed. 50% probability surfaces are shown.

porphyrin N$_P$–Fe–N$_P$ angles; the pyridine planes make dihedral angles, ϕ, of 35° and 36° to the closest Fe–N$_P$ axis. The dihedral angles between the pyridine planes and the mean porphyrin core are 86.9° and 86.6°. The dihedral angles between the phenyl rings and the mean porphinato core are 58.5°, 67.0°, 60.6°, and 60.9°.

Individual values of bond distances and angles for [Fe(TPP)-(4-CNPy)$_2$]ClO$_4$ are given in Tables 2 and 3. Averaged values for the chemically equivalent bond distances and angles for the complex are shown in Figure 2; distances and angles within the porphyrin core are not remarkable. The equatorial Fe–N$_P$ bond distances average to 1.952(7) Å, which is the shortest distance so far reported[43] for any bis(pyridine)iron(III) porphyrinate derivative. These short Fe–N$_P$ distances are consistent with the extreme S$_4$ ruffling of the core, which is the most extensively ruffled porphyrin core among known bis(pyridine)iron(III) porphyrinates.[43] Individual values of displacements of the crystallographically unique atoms from the mean plane of the 24-atom core (in units of 0.01 Å) are shown in Figure 2. Another measure of the strong S$_4$ ruffling is shown by the bending of the methine carbon atoms out of the plane of the individual pyrrole rings by an average of ±0.18 Å. The two independent axial bond distances are 1.997(4) and 2.008(4) Å. The axial N–Fe–N angle is 178.61(16)°, and the N$_{ax}$–Fe–N$_P$ angles range from 91.72 (16) to 89.15 (15)°. The coordination group geometry is thus seen to deviate by a small but significant amount from that of the ideal C$_{4v}$ point group.

The Mössbauer spectra of polycrystalline [Fe(TPP)(4-CNPy)$_2$]-ClO$_4$ taken at 120 K and 4.2 K are shown in Figure 3. The 4.2 K spectrum shows broad wings extending beyond ±5 mm/s which must originate from partially averaged magnetic hyperfine interaction. The 120 K spectrum consists of a somewhat broadened quadrupole doublet with a splitting of ΔE_Q = 0.65(1) mm/s and isomer shift δ_{Fe} = 0.19(1) mm/s. The solid line in Figure 3a represents a fit with Voigt line shape,[38] which fits better than a Lorentzian. The isomer shift is typical for low-spin ferric hemes,[2,5,6,44] but the quadrupole splitting is unusually small. Values of ~1.75 mm/s are expected for low-spin iron(III) porphyrinates with perpendicular axial ligand orientations and a "pure" (d$_{xy}$)^2-(d$_{xz}$,d$_{yz}$)^3 ground state,[2,5,6] and values greater than ~2.00 mm/s are expected for derivatives with relative parallel ligand orientations.[2,5] A small value is also observed for the analogous TMP complex, [Fe(TMP)(4-CNPy)$_2$]ClO$_4$, (0.97 mm/s),[6] but the quadrupole splitting of the present TPP complex is much smaller. Like the corresponding TMP complex,[6] [Fe(TPP)(4-CNPy)$_2$]-

Table 2. Bond Distances in [Fe(TPP)(4-CNPy)$_2$]ClO$_4$·CH$_2$Cl$_2$[a]

type	length, Å	type	length, Å
Fe–N(1)	1.950(4)	C(12)–C(13)	1.392(7)
Fe–N(2)	1.957(4)′	(C13)–C(14)	1.377(8)
Fe–N(3)	1.944(4)	C(14)–C(15)	1.376(7)
Fe–N(4)	1.958(4)	C(15)–C(16)	1.400(7)
Fe–N(5)	1.997(4)	C(16)–C(11)	1.399(7)
Fe–N(6)	2.008(4)	C(21)–C(22)	1.395(7)
N(1)–C(a1)	1.382(6)	C(22)–C(23)	1.377(7)
N(1)–C(a2)	1.376(6)	C(23)–C(24)	1.378(8)
N(2)–C(a3)	1.385(6)	C(24)–C(25)	1.370(8)
N(2)–C(a4)	1.376(6)	C(25)–C(26)	1.400(7)
N(3)–C(a5)	1.382(6)	C(26)–C(21)	1.388(7)
N(3)–C(a6)	1.376(6)	C(31)–C(32)	1.404(7)
N(4)–C(a7)	1.382(6)	C(32)–C(33)	1.387(7)
N(4)–C(a8)	1.383(6)	C(33)–C(34)	1.373(8)
N(5)–C(47)	1.344(6)	C(34)–C(35)	1.391(8)
N(5)–C(51)	1.351(6)	C(35)–C(36)	1.383(7)
N(6)–C(53)	1.343(6)	C(36)–C(31)	1.383(7)
N(6)–C(57)	1.332(6)	C(41)–C(42)	1.398(7)
C(a1)–C(b1)	1.431(6)	C(42)–C(43)	1.380(7)
C(a1)–C(m4)	1.393(6)	C(43)–C(44)	1.365(8)
C(a2)–C(b2)	1.431(7)	C(44)–C(45)	1.395(7)
C(a2)–C(m1)	1.396(6)	C(45)–C(46)	1.392(7)
C(a3)–C(b3)	1.424(7)	C(46)–C(41)	1.387(7)
C(a3)–C(m1)	1.391(7)	C(47)–C(48)	1.372(7)
C(a4)–C(b4)	1.444(6)	C(48)–C(49)	1.384(7)
C(a4)–C(m2)	1.392(6)	C(49)–C(50)	1.374(7)
C(a5)–C(b5)	1.431(7)	C(50)–C(51)	1.380(7)
C(a5)–C(m2)	1.398(7)	C(49)–C(52)	1.469(7)
C(a6)–C(b6)	1.427(7)	C(52)–N(7)	1.123(7)
C(a6)–C(m3)	1.404(6)	C(53)–C(54)	1.368(7)
C(a7)–C(b7)	1.446(7)	C(54)–C(55)	1.413(7)
C(a7)–C(m3)	1.383(7)	C(55)–C(56)	1.347(6)
C(a8)–C(b8)	1.432(7)	C(56)–C(57)	1.412(7)
C(a8)–C(m4)	1.393(7)	C(55)–C(58)	1.449(7)
C(b1)–C(b2)	1.357(6)	C(58)–N(8)	1.144(7)
C(b3)–C(b4)	1.342(7)	Cl(1)–O(1)	1.486(6)
C(b5)–C(b6)	1.336(7)	Cl(1)–O(2)	1.403(5)
C(b7)–C(b8)	1.336(7)	Cl(1)–O(3)	1.419(5)
C(m1)–C(11)	1.504(6)	Cl(1)–O(4)	1.479(5)
C(m2)–C(21)	1.496(7)	Cl(1)–O(5)	1.526(17)
C(m3)–C(31)	1.495(6)	Cl(1)–O(6)	1.208(21)
C(m4)–C(41)	1.492(7)	C(59)–Cl(2)	1.773(6)
C(11)–C(12)	1.390(7)	C(59)–Cl(3)	1.745(6)

[a] The estimated standard deviations of the least significant digits are given in parentheses.

ClO$_4$ displays an EPR spectrum that exhibits the large g_{max}[2,5,18] shape, but with an anomalously low single g-value (Figure 4), both in the solid polycrystalline state and in frozen solution. The observed g_{max} value in the polycrystalline solid state is 2.54, and that in solution is 2.57. As for [Fe(TMP)(4-CNPy)$_2$]ClO$_4$,[6] this g_{max} signal is identified as $g_\perp$ (= g_{xx} = g_{yy}) rather than as g_{zz}, as in the case of the g_{max} signal of [Fe(TMP)(4-NMe$_2$Py)$_2$]ClO$_4$.[5] The $g_\parallel$ (= g_{zz}) signal is apparently broadened and thus is not observed in either of these media. However, when a single crystal was rotated about an arbitrary axis, two nearly coincident signals whose positions varied slightly and two noncoincident signals whose positions varied strongly with the angle of rotation were observed. The positions of the four signals varied between the limits of 2.62 > g > 0.92. As the crystal was rotated and the strongly varying signals moved in turn to higher magnetic field (smaller g), the signal broadened significantly, as shown in Figure 5. Each of these signals was extremely difficult to detect in the region of the minimum g turning point at about 7500 G. Such extreme broadening is evidence of what is sometimes called "g-strain"[45] in this axial system, as will be discussed further below. A plot of the squares of the observed g-values as a function of the angle of rotation about the arbitrary axis is shown in Figure

(43) See Table X of ref 5 and formal diagram of the complexes [Fe(TMP)-(4-CNPy)$_2$]ClO4, [Fe(TMP)(3-ClPy)$_2$]ClO$_4$, and [Fe(TMP)(3-EtPy)$_2$]ClO$_4$ in ref 6.

(44) Debrunner, P. G. In *Iron Porphyrins, Part II*; Lever, A. B. P., Gray, H. B., Eds.; Addison-Wesley: Reading, MA, 1983; pp 161–249.

Table 3. Bond Angles in [Fe(TPP)(4-CNPy)₂]ClO₄·CH₂Cl₂[a]

type	value, deg	type	value, deg
N(1)FeN(2)	89.99(16)	C(a6)C(m3)C(a7)	121.7(4)
N(1)FeN(3)	178.24(16)	C(a6)C(m3)C(31)	118.0(4)
N(1)FeN(4)	90.17(16)	C(a7)C(m3)C(31)	119.9(4)
N(1)FeN(5)	91.72(16)	C(a8)C(m4)C(a1)	123.3(4)
N(1)FeN(6)	89.15(15)	C(a8)C(m4)C(41)	116.0(4)
N(2)FeN(3)	90.51(16)	C(a1)C(m4)C(41)	120.6(4)
N(2)FeN(4)	179.42(16)	C(m1)C(11)C(12)	123.1(5)
N(2)FeN(5)	89.55(16)	C(m1)C(11)C(16)	118.3(4)
N(2)FeN(6)	89.35(16)	C(12)C(11)C(16)	118.5(4)
N(3)FeN(4)	89.35(17)	C(11)C(12)C(13)	120.4(5)
N(3)FeN(5)	89.98(16)	C(12)C(13)C(14)	120.8(5)
N(3)FeN(6)	89.17(16)	C(13)C(14)C(15)	119.7(5)
N(4)FeN(5)	89.88(16)	C(14)C(15)C(16)	120.1(5)
N(4)FeN(6)	91.21(16)	C(11)C(16)C(15)	120.5(5)
N(5)FeN(6)	178.61(16)	C(m2)C(21)C(22)	120.5(4)
FeN(1)C(a1)	126.6(3)	C(m2)C(21)C(26)	121.0(4)
FeN(1)C(a2)	127.1(3)	C(22)C(21)C(26)	118.6(4)
C(a1)N(1)C(a2)	106.1(4)	C(21)C(22)C(23)	120.8(5)
FeN(2)C(a3)	127.5(3)	C(22)C(23)C(24)	120.2(5)
FeN(2)C(a4)	126.2(3)	C(23)C(24)C(25)	120.2(5)
C(a3)N(2)C(a4)	106.3(4)	C(24)C(25)C(26)	120.1(5)
FeN(3)C(a5)	126.9(3)	C(21)C(26)C(25)	120.2(5)
FeN(3)C(a6)	127.7(3)	C(m3)C(31)C(32)	121.2(4)
C(a5)N(3)C(a6)	105.1(4)	C(m3)C(31)C(36)	120.0(4)
FeN(4)C(a7)	127.2(3)	C(32)C(31)C(36)	118.8(4)
FeN(4)C(a8)	126.9(3)	C(31)C(32)C(33)	120.2(5)
C(a7)N(4)C(a8)	105.8(4)	C(32)C(33)C(34)	120.1(5)
FeN(5)C(47)	121.6(3)	C(33)C(34)C(35)	120.2(5)
FeN(5)C(51)	120.7(3)	C(34)C(35)C(36)	119.7(5)
C(47)N(5)C(51)	117.7(4)	C(31)C(36)C(35)	120.9(5)
FeN(6)C(53)	119.2(3)	C(m4)C(41)C(42)	119.0(5)
FeN(6)C(57)	121.6(3)	C(m4)C(41)C(46)	122.3(4)
C(53)N(6)C(57)	119.1(4)	C(42)C(41)C(46)	118.7(5)
N(1)C(a1)C(b1)	109.6(4)	C(41)C(42)C(43)	121.3(5)
C(b1)C(a1)C(m4)	125.4(4)	C(42)C(43)C(44)	120.0(5)
N(1)C(a1)C(m4)	124.6(4)	C(43)C(44)C(45)	119.7(5)
N(1)C(a2)C(b2)	109.9(4)	C(44)C(45)C(46)	120.7(5)
C(b2)C(a2)C(m1)	124.4(4)	C(41)C(46)C(45)	119.6(5)
N(1)C(a2)C(m1)	125.1(4)	N(5)C(47)C(48)	124.0(5)
N(2)C(a3)C(b3)	109.7(4)	C(47)C(48)C(49)	117.2(5)
C(b3)C(a3)C(m1)	125.9(4)	C(48)C(49)C(50)	120.3(5)
N(2)C(a3)C(m1)	123.8(4)	C(48)C(49)C(52)	119.8(5)
N(2)C(a4)C(b4)	108.7(4)	C(50)C(49)C(52)	119.9(5)
C(b4)C(a4)C(m2)	125.7(4)	C(49)C(50)C(51)	118.9(5)
N(2)C(a4)C(m2)	125.2(4)	C(50)C(51)N(5)	121.9(5)
N(3)C(a5)C(b5)	109.7(4)	C(49)C(52)N(7)	178.1(7)
C(b5)C(a5)C(m2)	126.3(4)	N(6)C(53)C(54)	121.9(4)
N(3)C(a5)C(m2)	123.6(4)	C(53)C(54)C(55)	119.1(4)
N(3)C(a6)C(b6)	110.5(4)	C(54)C(55)C(56)	119.5(5)
C(b6)C(a6)C(m3)	123.8(4)	C(54)C(55)C(58)	119.0(5)
N(3)C(a6)C(m3)	125.4(4)	C(56)C(55)C(58)	121.6(5)
N(4)C(a7)C(b7)	109.1(4)	C(55)C(56)C(57)	117.9(5)
C(b7)C(a7)C(m3)	125.5(4)	C(56)C(57)N(6)	122.6(5)
N(4)C(a7)C(m3)	124.9(4)	C(55)C(58)N(8)	179.2(7)
N(4)C(a8)C(b8)	109.8(4)	O(1)Cl(1)O(2)	104.8(4)
C(b8)C(a8)C(m4)	125.3(4)	O(1)Cl(1)O(3)	108.0(4)
N(4)C(a8)C(m4)	124.5(4)	O(1)Cl(1)O(4)	104.4(3)
C(a1)C(b1)C(b2)	107.2(4)	O(1)Cl(1)O(5)	153.7(7)
C(a2)C(b2)C(b1)	107.1(4)	O(1)Cl(1)O(6)	37.3(10)
C(a3)C(b3)C(b4)	107.3(4)	O(2)Cl(1)O(3)	111.7(3)
C(a4)C(b4)C(b3)	107.9(4)	O(2)Cl(1)O(4)	113.1(3)
C(a5)C(b5)C(b6)	107.7(4)	O(2)Cl(1)O(5)	85.2(7)
C(a6)C(b6)C(b5)	107.0(4)	O(2)Cl(1)O(6)	133.5(11)
C(a7)C(b7)C(b8)	107.6(4)	O(3)Cl(1)O(4)	113.9(3)
C(a8)C(b8)C(b7)	107.5(4)	O(3)Cl(1)O(5)	89.9(7)
C(a2)C(m1)C(a3)	123.2(4)	O(3)Cl(1)O(6)	107.1(10)
C(a2)C(m1)C(11)	115.1(4)	O(4)Cl(1)O(5)	49.7(7)
C(a3)C(m1)C(11)	121.6(4)	O(4)Cl(1)O(6)	70.9(11)
C(a4)C(m2)C(a5)	123.9(4)	O(5)Cl(1)O(6)	119.7(12)
C(a4)C(m2)C(21)	118.6(4)	Cl(2)C(59)Cl(3)	112.2(3)
C(a5)C(m2)C(21)	117.4(4)		

[a] The estimated standard deviations of the least significant digits are given in parentheses.

6. It was difficult to find *single* crystals of a size appropriate for single crystal EPR investigations, and the crystal from which the data presented in Figures 5 and 6 were obtained shattered after
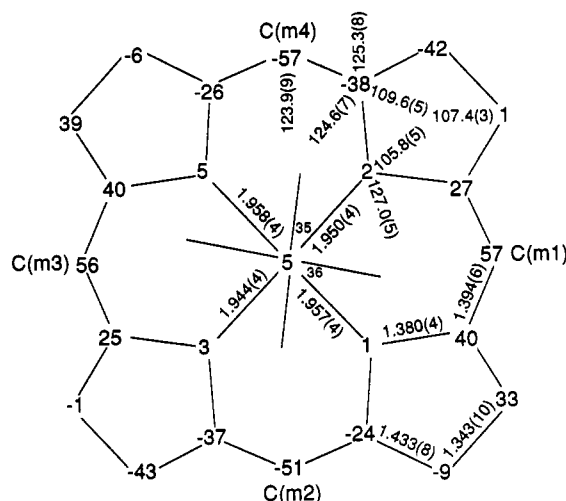

Figure 2. Formal diagram of the porphinato core in [Fe(TPP)(4-CNPy)₂]-ClO₄. Deviations of each unique atom from the mean plane of the core (in units of 0.01 Å) are shown. Averaged values for the chemically unique bond distances and angles in the core are also shown. The orientation of the axial ligand planes with the closest Fe–Np vector (angle ϕ) are shown. Individual values of the Fe–Np bond distances are shown.

the series of orientations about the arbitrary axis shown in Figure 6 were obtained, following warming to room temperature. Other mounted crystals showed multiple (more than four) signals, all within the g-value range observed for the single crystal (Figure 6). For this reason and the possibility of spin exchange between closest pairs of magnetic centers in the unit cell, it was not possible to determine the true maximum and minimum g-values or to establish unequivocally their absolute orientation with respect to the porphyrin plane and pyridine axes of the complex. However, because there are four molecules per unit cell whose relative orientations *are* known, *i.e.*, the angles of the porphyrin planes of the four molecules (1/4 = 76.77°, 1/3 = 70.92°, 1/2 = 63.62°), the rotation behavior shown in Figure 6 tentatively defines 1 and 2 as being the strongly varying signals and 3 and 4 as being the slightly varying signals. It is clear that the true maximum and minimum g-values are not far different from 2.62 and 0.92, respectively.

For comparison of the crystal and molecular structure discussed above to that obtained from molecular mechanics calculations that would allow estimation of the barrier to rotation of the axial ligands, MM2* calculations were carried out on [Fe(TPP)(Py)₂]⁺, using the structure determined by Strouse and co-workers.[10] Figure 7 shows an overlay of the crystal conformation of [Fe(TPP)-(Py)₂]Cl[10] with the MM2* minimized structure. It is evident that the energy minimization does not bring about significant distortions in the geometry of the TPP ligand. The major changes involve a slight flattening of the porphyrin as well as a "straightening" of the axial ligands so that they are orthogonal to the porphyrin plane, as shown in Figure 7, where the observed structures are more ruffled than the calculated ones. In the crystal structure, the axial ligands are not orthogonal to the plane of the porphyrin, possibly due to crystal packing forces. Figure 7b shows a similar overlay for [Fe(TMP)(4-NMe₂Py)₂]⁺.[5] In this case, the flattening of the porphyrin is much more drastic, and once again, the minimization has "orthogonalized" the axial ligands.

In order to determine the barrier to rotation of pyridine ligands, both axial ligands were rotated in 10° increments, in phase, so as to maintain a constant 90° dihedral angle between the planes of the pyridines. The torsional barrier about the iron–pyridine nitrogen bond was set at 500 kcal/mol in order to insure that the orientation of the planes of the axial ligands with regard to the location of the pyrrole nitrogens would remain constant while minimization occurred in the remainder of the molecule. The barrier to rotation of the axial ligands calculated in this manner

Axial Ligand Orientation in Iron(III) Porphyrinates

J. Am. Chem. Soc., Vol. 116, No. 17, 1994   7765
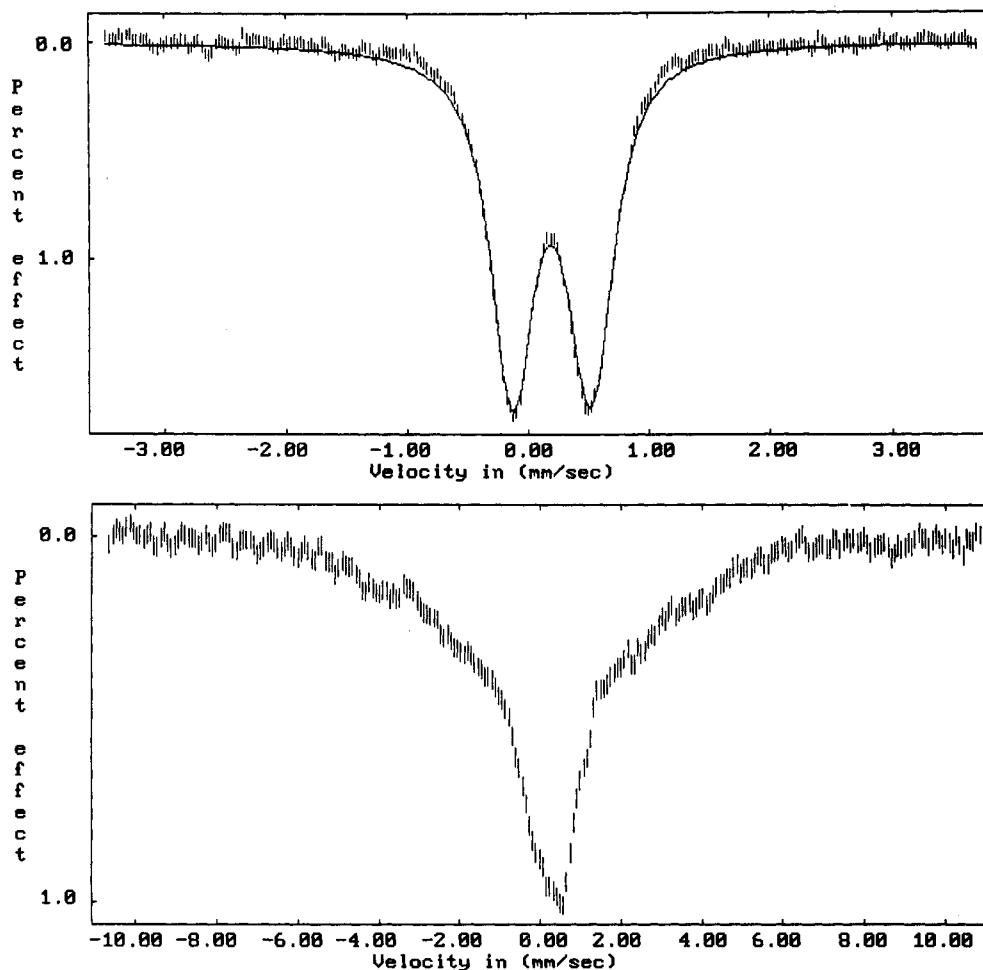
Figure 3. Mössbauer spectra of polycrystalline [Fe(TPP)(4-CNPy)$_2$]ClO$_4$ in a field of 220 mT perpendicular to the γ-beam (a, top) at 120 and (b, bottom) at 4.2 K. The solid line in spectrum a is a fit with two Voigt lines[38] of equal areas, quadrupole splitting ΔE_Q = 0.65 mm/s, and isomer shift δ_{Fe} = 0.19 mm/s.
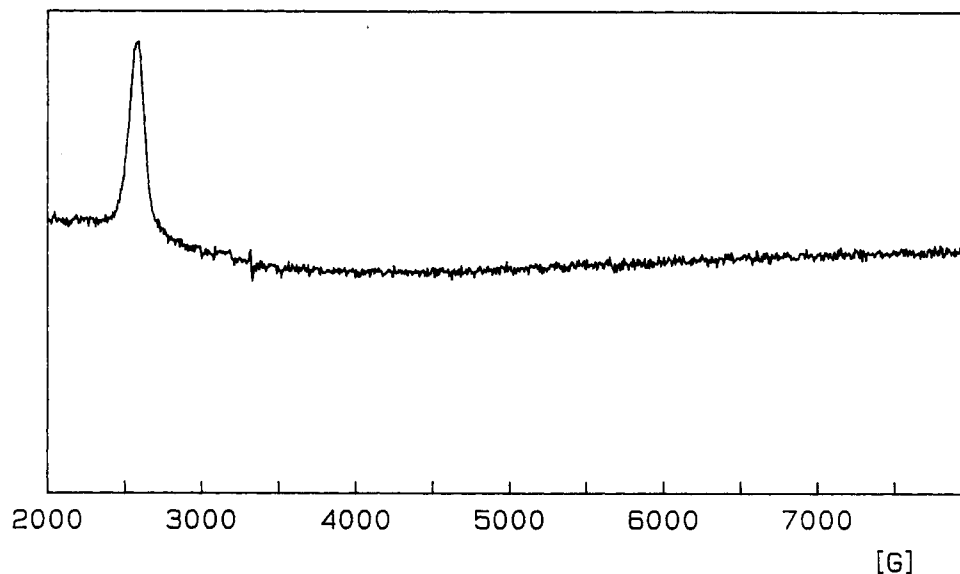

Figure 4. EPR spectrum of a frozen solution of [Fe(TPP)(4-CNPy)$_2$]ClO$_4$ in methylene chloride, recorded at 4.2 K. Note that there is no evidence of the $g_\parallel$ signal near 7500 G. In addition, there are not signals at lower magnetic field (larger g-value) than shown herein.

is thus the maximum possible barrier. As can be seen in Figure 8, the barrier to rotation calculated under these conditions is approximately 2.2 kcal/mol for both the TPP and the porphine ligands and smaller (~0.9 kcal/mol) for the TMP ligand. The TPP and porphine systems, however, are at identically lower overall energies than the TMP system. In each case, the energy is at a maximum when the planes of the pyridine ligands eclipse then N$_P$–Fe–N$_P$ axes. The structures of the complexes represented by the data points for the barriers to rotation of the axial pyridine ligands have been used to prepare an animation of the porphyrin ring deformation that takes place during the rotation process, which is available on anonymous FTP or diskette.[46]

(45) (a) More, C.; Bertrand, P.; Gayda, J. P. *J. Magn. Reson.* **1987**, *73*, 13. (b) More, C.; Gayda, J. P.; Bertrand, P. *Ibid.* **1990**, *90*, 486.
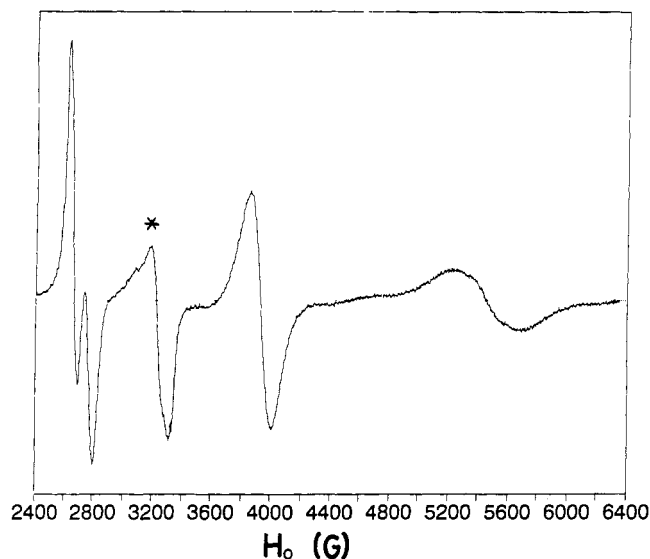
Figure 5. Single crystal EPR spectrum of [Fe(TPP)(4-CNPy)₂]ClO₄ at 4.2 K at an arbitrary rotation angle chosen to illustrate the severe broadening of the signals having small g-value. The signal marked with the asterisk near 3200 G is due to a copper oxide impurity in the liquid helium dewar, which was discovered after these experiments were completed. It shows no change in position as a function of angle.

Discussion

Structure of the Complex. [Fe(TPP)(4-CNPy)₂]ClO₄ is another example of a bis(pyridine)(porphyrinato)iron(III) complex in which the axial ligands are in perpendicular planes lying over the meso positions of the porphyrin ring, which in turn has a strongly ruffled conformation. The average displacement of the meso carbons is ±0.55 Å, even though no o-methyl groups are present on the phenyl rings, as was the case for the series of [Fe(TMP)(L)₂]ClO₄ (±0.36–0.51 Å), where L is 4-NMe₂Py,[5] 3-EtPy,[6] 3-ClPy,[6] or 4-CNPy.[6] In the tetramesityl series, it was suggested that interacton of the axial ligands with the 2- and 6-methyl substituents might contribute to the observed ruffling of the porphyrinato core.[5,6] However, there is no apparent steric reason why the present (tetraphenylporphyrinato)iron(III) complex should be as ruffled as the TMP analogs. The fact that

[Fe(TPP)(4-CNPy)₂]ClO₄ is even *more* ruffled than [Fe(TMP)-(4-CNPy)₂]ClO₄ points to electronic effects being more important in causing the observed ruffling than steric effects.

In Table 4 are summarized the average absolute value of the methine carbon atom displacement, a measure of core ruffling, and the average Fe–Nₚ bond distance for the 13 (porphyrinato)-iron(III) derivatives of known structure that have either a large g_{max} or an axial EPR spectrum. As noted in the Introduction, the large g_{max} EPR features means that these derivatives have a nearly degenerate d$_\pi$ (d$_{xz}$,d$_{yz}$) pair. The same is true for the complexes that have axial EPR spectra, but these complexes additionally have the d$_{xy}$ orbital lying above the d$_\pi$ pair in energy. This clearly distinguishes them from the majority of low-spin iron(III) porphyrinates which have an x,y rhombic electronic state. Entries of Table 4 are ordered on the basis of the Fe–Nₚ bond distances. These distances are seen, with one exception, to be shorter than the 1.990-Å value typically observed for low-spin (rhombic) (porphyrinato)iron(III) derivatives;[47] all known iron-(III) derivatives with short Fe–Nₚ bonds are members of the class. We believe that short Fe–Nₚ bonds are observed in these derivatives because the iron electronic structure is more favorable for strong Porph→Fe π-bonding. The near degeneracy of the iron d$_\pi$ pair should lead to more equivalent and probably stronger π interaction between the four nitrogen atoms of the porphyrin ring and iron; the strength of this interaction clearly depends on both the energy level and the effective population of the d$_\pi$ orbitals. When the axial ligands are reasonably strong Lewis bases (good σ-donors), the two d$_\pi$ orbitals have a single vacancy that is approximately equally shared and should be able to equally accept π electron density from the porphyrin in the x and y directions. When the axial ligands are strong π-acceptors, such as 4-cyan-opyridine, the energy of the d$_\pi$ orbitals is decreased relative to d$_{xy}$, and thus both d$_\pi$ orbitals are filled. However, in this case iron(III) must strongly π-donate electron density to the axial ligands, and it is thus better able to be a good π-acceptor from the π-donating porphyrin ligand. The increased Fe–Nₚ π-bonding thus engendered should lead to shorter bond distances. However, the macrocyclic constraints of the porphyrin ligand do not allow a simple ring contraction; rather, shortened Fe–Nₚ bonds must also be accompanied by ring ruffling, as was first noted by
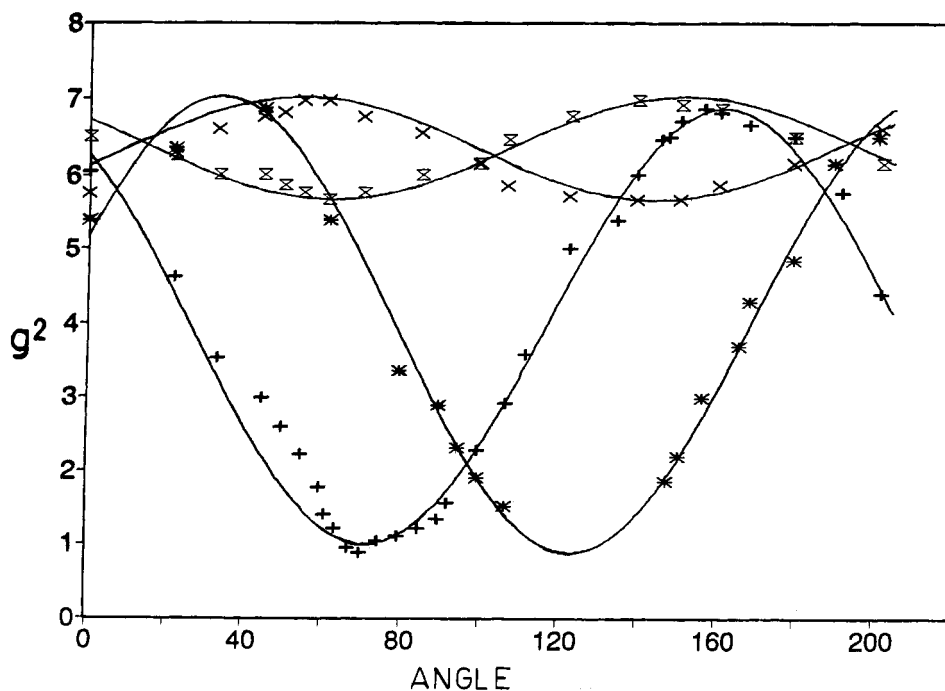
Figure 6. Plot of (g$_{obs}$)² vs angle θ of rotation about an arbitrary axis of the crystal of [Fe(TPP)(4-CNPy)₂]ClO₄.
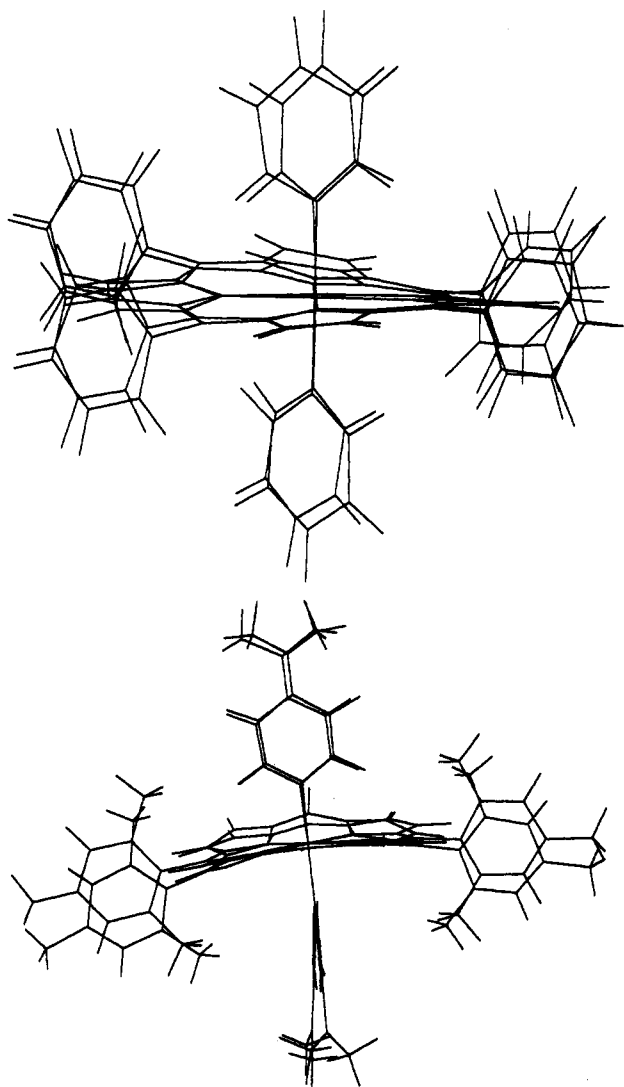
Figure 7. (a, top) Energy-minimized structures of [Fe(TPP)(Py)$_2$]$^+$, compared to the reported molecular structure of the same ion;[10] (b, bottom) energy-minimized structure of [Fe(TMP)(4-NMe$_2$Py)$_2$]$^+$, compared to the reported molecular structure of the same ion.[5] In each case, the observed molecular structure has the more ruffled porphyrin plane, which places the phenyl groups further below or above the plane than is predicted by the energy-minimized structure. Also, in each case, the axial ligands are further off the normal to the mean plane of the porphyrin in the observed than in the energy-minimized structures. For structure b, two of the phenyl rings have been omitted from the observed and calculated structures for clarity.

Hoard.[48,49] It is to be expected that the shorter the bond, the greater the ruffling, and the entries of Table 4 are seen to follow this general trend. The shortening of up to 0.04 Å is a bit larger than was seen for comparable core ruffling (±0.60 Å) in a cobalt-(III) derivative,[50] when the Co–N$_P$ shortening is ~0.02–0.03 Å.

The difference in the structures of the two bis(cyano) complexes of Table 4 suggests that the intrinsic energetic barrier to core ruffling might also play a role in the interplay between π-bonding and ring ruffling, *i.e.*, the energetics of ring ruffling and enhanced

(46) The animation can be obtained directly from the ACS (see Supplementary Material Available paragraph) or by anonymous FTP from joplin .biosci.arizona.edu, in the /pub/porphmovie directory. Minimum computer hardware requirements for playing this "movie" are Macintosh computer running at least system 7.0 and a quicktime system extension or an IBM-compatible PC running Microsoft Windows 3.1.

(47) Scheidt, W. R.; Reed, C. A. *Chem. Rev.* **1981**, *81*, 543.

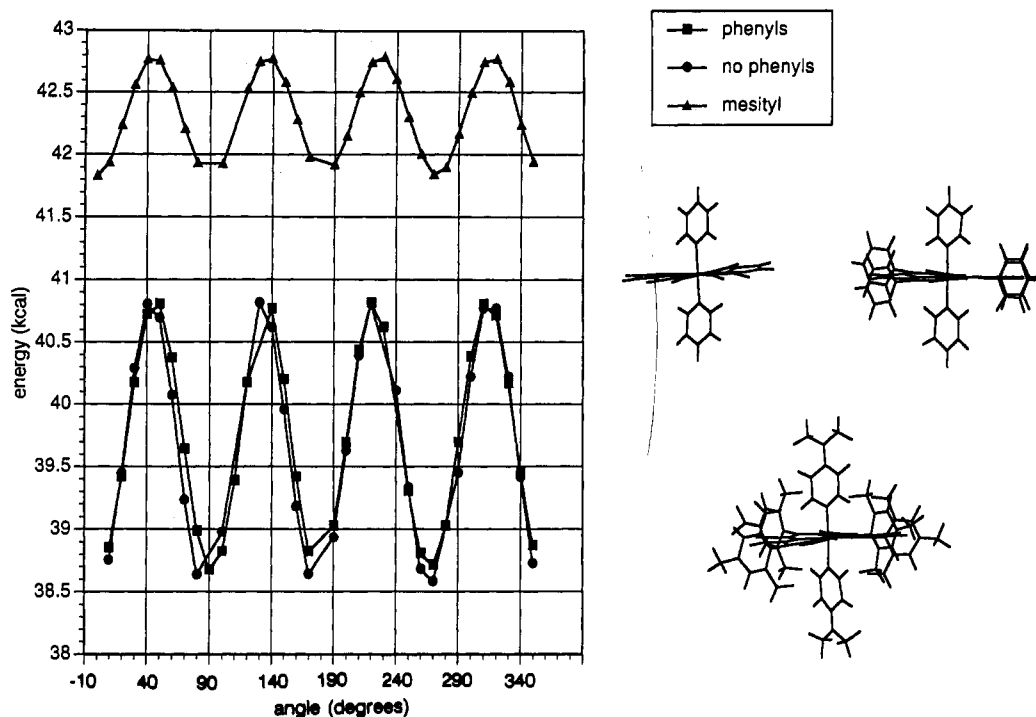(48) Hoard, J. L. *Ann. N. Y. Acad. Sci.* **1973**, *206*, 18.

(49) Collins, D. M.; Scheidt, W. R.; Hoard, J. L. *J. Am. Chem. Soc.* **1972**, *94*, 6689.

(50) Kaduk, J. A.; Scheidt, W. R. *Inorg. Chem.* **1974**, *13*, 1875.

bonding are roughly comparable. The two bis(cyano) complexes are seen to have the shortest[51] and longest[52] Fe–N$_P$ bond distances, with ruffled and planar cores, respectively. The complex [Fe(handle)CN)$_2$]$^-$ was synthesized[51] with a short strap across each face of the porphyrin in order to spatially limit the volume available for axial ligand binding and to thus "kink" the bound cyanide ligand. An effect that was not necessarily in the porphyrin ligand design is that the short straps also favor ruffling of the core, and the increase in strain energy upon ruffling is less than that of the TPP derivative.

A recent molecular mechanics (MM) study of the S_4 ruffling of metal complexes of porphine in the absence of axial ligands has shown that MM techniques can be used to predict the structure of metalloporphyrins containing a wide range of sizes of metal ion and hence the extent of porphyrin core ruffling.[42] It was found that for Fe(III) porphyrins, a planar core is always more stable than a ruffled core, although the calculated differences are small, and hence metalloporphyrins "...are therefore capable of adopting a variey of conformations in response to such factors as the orientation of axial ligands and the interaction with their environment." [42]

Mössbauer and EPR Spectra. It is clear from both the extremely small Mössbauer quadrupole splitting (0.65 nm/s) and the EPR g-values ($g_\perp \geq 2.62$, $g_\parallel \leq 0.92$) that [Fe(TPP)(4-CNPy)$_2$]-ClO$_4$ is the most extreme case of stabilization of the $(d_{xz},d_{yz})^4$-$(d_{xy})^1$ ground state at very low temperatures reported thus far for bis(pyridine) complexes of Fe(III) porphyrinates. Utilizing the proper axis definition of Taylor ($V/\Delta \leq 2/3$),[26] we define g_{zz} = -0.92, g_{yy} = 2.62, and g_{xx} = -2.62, which leads to a calculated tetragonality parameter, Δ/λ = -1.72. The negative sign indicates that d_{xy} is higher in energy than the degenerate d_{xz},d_{yz} pair. We also find that the mixing coefficients a, b, and c, for the wave functions of d_{xz}, d_{yz} and d_{xy}, respectively, are a = 0.289, b = 0.289, c = 0.891; thus c^2 = 0.794 and $a^2 + b^2 + c^2$ = 0.962, indicating the need for an orbital reduction factor, k = 1.04. The orbital of the unpaired electron is thus 82.5% d_{xy} in character. Note the sum of the squares of the apparent g-values, $\Sigma(g_{app})^2$ = 14.58. This value is considerably less than the theoretical maximum of 16 predicted for a "pure" $(d_{xy})^2(d_{xz},d_{yz})^3$ ground state.[25] The deviation of the Σg^2 from the theoretical limit of 16 and the decrease in the Mössbauer quadrupole splitting constant are both indicative of partial quenching of orbital angular momentum in the ground-state electron configuration of the complex, as is expected as the percentage of d_{xy} character of the orbital of the unpaired electron increases. In the limit of a "pure" $(d_{xz},d_{yz})^4(d_{xy})^1$ ground state, with no contribution to the wave function of the unpaired electron due to spin–orbit coupling with d_{xz} and d_{yz} (*i.e.*, $a = b = 0$, $c = 1$), we expect to find that g_{xx} = g_{yy} = g_{zz} = 2, and that an isotropic EPR signal similar to those of organic free radicals would be observed. In this limit, then, Σg^2 = 12. This limit has been approached most closely to date in the case of [Fe(TPP)(*t*-BuNC)$_2$]ClO$_4$ ($g_\perp$ = 2.19, $g_\parallel$ = 1.94; Σg^2 = 13.36),[33] though the [Fe(OEC)(*t*-BuNC)$_2$]$^+$ complex (OEC = octaethylchlorin), which was previously formulated as a π cation radical complex of Fe(II),[53] may actually be another example of a nearly pure $(d_{xz},d_{yz})^4(d_{xy})^1$ ground-state complex.

In order to understand why only the $g_\perp$ feature of the axial EPR signal of [Fe(TPP)(4-CNPy)$_2$]ClO$_4$ is resolved, we have considered how the calculated tetragonality, Δ/λ,[17,25,26] varies with changes in $g_\perp$ and $g_\parallel$ as a function of Σg^2. In Figure 9 is shown a plot of Δ/λ as a function of $g_\perp$ and $g_\parallel$ for Σg^2 = 12.0–16.0 in increments of 1.0. As is obvious, for $g_\perp$ = 2.62, the calculated value of $g_\parallel$ varies strongly, from 0.52 (Σg^2 = 12) to 1.51 (Σg^2 = 16), while $|\Delta/\lambda|$ varies over the relatively smaller relative range of 1.35–2.64. In fact, for any given value of Σg^2,

(51) Schappacher, M.; Fischer, J.; Weiss, R. *Inorg. Chem.* **1989**, *28*, 389.

(52) Scheidt, W. R.; Haller, K. J.; Hatano, K. *J. Am. Chem. Soc.* **1980**, *102*, 3017.

(53) Sullivan, E. P.; Strauss, S. H. *Inorg. Chem.* **1989**, *28*, 3093.

Figure 8. Calculated barrier to rotation of two pyridine ligands when rotated by 10° increments in phase while maintaining a constant 90° angle between their planes. (The angles 0°, 90°, 180°, and 270° are defined as the positions when the projected planes of the pyridine ligands bisect the N_P–Fe–N_P axes.) As can be seen, the calculated barrier to rotation is approximately 2.2 kcal for Fe^{III}(porphine) (●) and Fe^{III}(TPP) (■) and somewhat less (~0.9 kcal) for Fe^{III}(TMP) (▲).

Table 4. Summary of Geometrical Parameters for Low-Spin (Porphyrinato)iron(III) Derivatives with Large g_{max} or Axial EPR Spectra

complex	Fe–Np, Å[a]	Fe–N_{ax}, Å	C_m displ[b]	ref
[Fe(TPP)(CN)₂]⁻	2.000(6)		4[c]	51
[Fe(TPP)(Py)₂]⁺	1.982(7)	2.003(3)	25	10
[Fe(OEP)(CN)(Py)]	1.980(4)	2.087(3)	29	d
[Fe(T2,6Cl₂PP)(1-VinIm)₂]⁺	1.976(8)	1.972(6)	22[e]	4
[Fe(TPP)(CN)(Py)]	1.970(14)	2.075(3)	38	f
[Fe(TPP)(2-MeHIm)₂]⁺	1.970(4)	2.012(4)	39	3
[Fe(TMP)(3-ClPy)₂]⁺	1.968(2)	2.012(8)	36	6
[Fe(TMP)(4-NMe₂Py)₂]⁺	1.964(10)	1.984(8)	51	5
[Fe(TPP)(Ph)]	1.961(7)		11[g]	h
[Fe(TMP)(4-CNPy)₂]⁺	1.961(7)	2.011(14)	41	6
[Fe(TMP)(3-EtPy)₂]⁺	1.961(4)	2.000(9)	43	6
[Fe(TPP)(4-CNPy)₂]⁺	1.952(7)	2.002(8)	55	this work
[Fe(handle)(CN)₂]⁻	1.949(14)		64	50

[a] The number in parentheses is the estimated standard deviation of the averaged value. *[b]* Averaged value of *meso*-carbon atom displacement from the porphyrin ring in units of 0.01 Å. Except where noted, all derivatives have a "ruf" core conformation. *[c]* Planar core. *[d]* Scheidt, W. R.; Hatano, K. *Acta Crystallogr.* **1991**, *C47*, 2201. *[e]* Species is mixture of parallel and perpendicular axial ligand geometries. *[f]* Scheidt, W. R.; Lee, Y. J.; Luangdilok, W.; Haller, K. J.; Anzai, K.; Hatano, K. *Inorg. Chem.* **1983**, *22*, 1516. *[g]* "Sad" conformation; solid-state dimers. *[h]* Doppelt, P. *Inorg. Chem.* **1984**, *23*, 4009.

representing a particular degree of quenching of spin–orbit coupling, a small change in $g_\perp$ leads to a larger change in $g_\|$, but only a very small change in Δ/λ, as shown in Figure 9, at least until both g-values closely approach 2.0. Added to this larger variation in $g_\|$ is the effect of the inverse relationship between g-values and magnetic field. Thus, any ligand vibrations that slightly affect the value of Δ/λ will cause a large change in the associated value of $g_\|$, thus making the position of the parallel feature in the EPR spectrum uncertain. This uncertainty leads to excessive broadening of the parallel feature of the EPR spectrum.[45] From inspection of Figure 9, it becomes clear that this excessive broadening can occur for the axial EPR spectra of a $(d_{xz},d_{yz})^4(d_{xy})^1$ ground-state system, just as it does for the rhombic spectra of $(d_{xy})^2(d_{xz},d_{yz})^3$ ground-state systems.[45]

NMR Spectral Features. Some years ago, La Mar and co-workers investigated in detail the NMR spectra of a series of bis(*p*-substituted-pyridine) complexes of Fe^{III}(TPP).[28] They found that the pyrrole-H resonance of the TPP ligand shifts to higher frequency (δ_{iso} decreases in magnitude), while the isotropic shift of the phenyl-H resonances increase in an alternating fashion (δ_{iso}(*o*-H,*p*-H) negative, δ_{iso}(*m*-H) positive) as the basicity of the pyridine decreases. The decreasing magnitude of the pyrrole-H isotropic shifts with decreasing basicity of the axial ligands was more recently also observed for the corresponding tetramesitylporphyrinate complexes, where it was possible to show that it was due to a progressive change in the electronic ground state from largely $(d_{xy})^2(d_{xz},d_{yz})^3$ to largely $(d_{xz},d_{yz})^4(d_{xy})^1$ as the basicity of the axial pyridine ligand decreases.[6] However, the increasing shfts of the *meso*-phenyl resonances with decreasing ligand basicity, originally ascribed to increasing π delocalization to the meso carbon positions,[28] were reinterpreted as indicating partial delocalization to the meso positions by means of the parial (d_{xz},d_{yz}) character of the unpaired electron, even when the electron was largely localized in the d_{xy} orbital.[6] More recently, however, we have shown that the size of the contact shift expected from this mechanism is too small to account for the observed isotropic shifts of the phenyl protons of [Fe(TPP)(4-CNPy)₂]ClO₄ and related complexes.[30] Hence, the large π spin delocalization to the meso positions suggest at least partial porphyrin π cation radical character to the electron configurations of these complexes.[30] The limit of this π cation radical character is to convert the electron configuration to that of Fe(II)(P•⁻).[53] We have observed that Fe(III) porphyrinates that have a $(d_{xz},d_{yz})^4(d_{xy})^1$ ground state invariably appear to be pushed toward having partial porphyrin π cation radical character (in terms of both their EPR and NMR spectra), even though the d_{xy} orbital is orthogonal to the π orbitals of the porphyrin ring. The reasons for this behavior are probably related, at least in part, to the invariably observed strong S_4 ruffling of the porphinato core[5,6,33] in systems having a predominantly $(d_{xz},d_{yz})^4(d_{xy})^1$ ground state, as discussed further below.
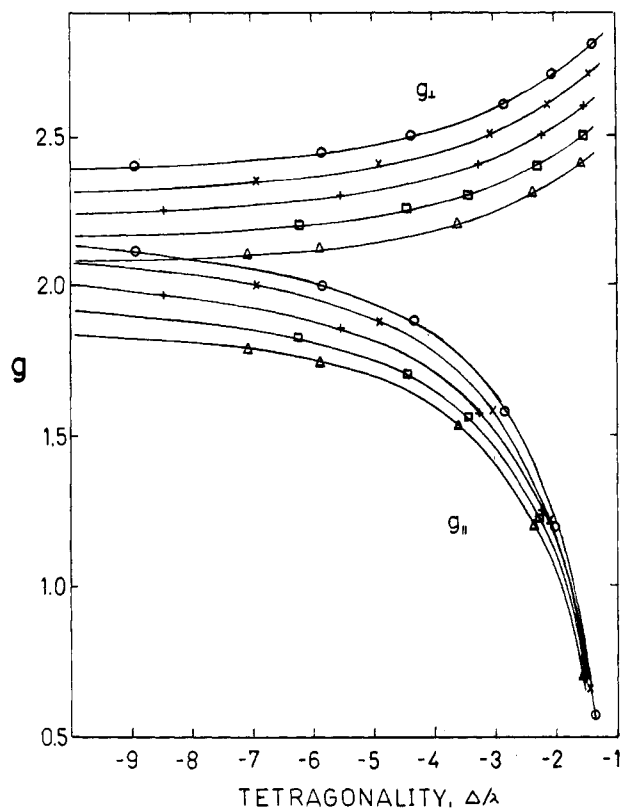
Figure 9. Plot of the g-values ($g_\parallel < 2 < g_\perp$, where $g_\perp$ is varied in units of 0.1) *vs* the tetragonality parameter, Δ/λ, for low-spin Fe(III) porphyrinates having a predominantly $(d_{xz},d_{yz})^4(d_{xy})^1$ ground state for different values of Σg^2: $\triangle$ 12; $\square$ 13; + 14; $\times$ 15; $\bigcirc$ 16. (Tetragonality is a measure of the field strength of the ligands. The negative values of Δ/λ indicate that d_{xy} is higher than d_{xz} and d_{yz}.) Note that as Σg^2 is increased, $g_\parallel$ varies much more strongly than $g_\perp$, as the magnitude of the tetragonality increases.

Molecular Mechanics Calculations. There have been a number of investigations of the tendency of metal complexes of the reduced hemes (chlorins and isobacteriochlorins) and Factor F430 to deform from planarity in a manner that is described in terms of the group theory of a symmetrical porphyrin ring as either S_4-saddle (sad) or S_4 ruffled (ruf). In S_4-saddle deformation, opposite pyrrole rings, and hence metal–porphyrin nitrogen bonds, are displaced from planarity, creating a pseudotetrahedral distortion in the metal coordination. In contrast, in S_4-ruffled structures, opposite pyrrole rings are counterrotated about the metal–nitrogen bonds such that the metal and the four porphyrin nitrogens are in a plane, but the meso carbons and the β-pyrrole carbons are displaced from this plane in an up–down alternating fashion.[42] As is evident from Figures 1, 2, and 7 and the data of ref 5 and 6, [Fe(TPP)(4-CNPy)$_2$]ClO$_4$ and related complexes exhibit S_4 ruffling. It has been generally accepted for some time that the ease of ruffling generally increases in the order porphyrins < chlorins < isobacteriochlorins < F430.[54–56] However, it is now becoming clear that porphyrins may deform from planarity much more easily than assumed heretofore. Our own MM2* calculations confirm this and further show that the phenyl rings of the tetraphenylporphyrinate ligand contribute nothing in terms of the barrier to rotation of two perpendicularly aligned axial ligands, as shown in Figure 8.[46] The more shallow barrier to rotation calculated for the TMP complex is due to a destabilization of the

valleys caused by a van der Waals repulsion between the pyridine ligands and the o-methyl groups of the TMP rather than a stabilization of the conformation in which the pyridine planes eclipse the N$_P$–Fe–N$_P$ axes. Our calculations also suggest that if the barrier to rotation of pyridine ligands is as small as indicated by the calculations (2.2 kcal/mol for the TPP complex and 0.9 kcal/mol for the TMP complex), it is highly unlikely (1) that pyridine ligand rotation is slow on the NMR time scale at –70 °C, as suggested previously,[57] and (2) that the axial pyridine ligands of [Co(TPP)(Py)$_2$]$^+$ are prevented from rotating at ambient temperatures in solution, as concluded previously.[58]

The *observed* degree of ruffling found in the structures of the low-spin Fe(III) porphyrinates bound to low-basicity pyridines is somewhat larger in the case of the TPP ligand (Figure 7a) and considerably larger in the case of the TMP ligand (Figure 7b) than predicted by the molecular mechanics calculations. This suggests that there is in reality an additional energy contribution to ruffling that is not included in the MM2* calculations, an *electronic* factor that may favor the ruffled conformation. *For six-coordinate low-spin Fe(III) porphyrinates having the $(d_{xz},d_{yz})^4(d_{xy})^1$ ground state*, this electronic factor must involve the single occupancy of the d_{xy} oribtal and should, at the same time as it explains the S_4 ruffling, provide an explanation of the large amount of π unpaired electron density observed at the meso positions of complexes such as [Fe(TPP)(4-CNPy)$_2$]$^+$ [28] and its TMP analog.[6] The pattern of spin delocalization observed in those low-spin Fe(III) porphyrinates having the $(d_{xz},d_{yz})^4(d_{xy})^1$ ground state is suggestive of spin delocalization into the valence $a_{2u}(\pi)$ orbital of the porphyrin ring, which has large electron density at the four porphyrin nitrogens and at the four meso positions but nearly zero electron density at the β-pyrrole positions.[59] An *unlikely* possibility is that although the d_{xy} orbital is orthogonal to the π orbitals of the porphyrin ring when it is planar, the two positive lobes of the $a_{2u}(\pi)$ orbital at opposite meso positions can overlap with the two positive lobes of the d_{xy} orbital, while the two negative lobes at the other two meso positions can overlap with the two negative lobes of the d_{xy} orbital when the porphyrin ring is strongly S_4-ruffled so that the meso positions are alternately above and below the mean plane of the porphyrin. This would allow P→Fe π back-bonding to occur and produce the observed tendency (in terms of both NMR shifts and EPR g-values) toward π cation radical character. It would also tend to reinforce the tendency toward S_4 ruffling. However, the ~3.5-Å distance between the metal and the meso carbons is too large for significant orbital overlap, and in addition, the S_4 ruffling would tip the p$_z$ orbitals of the meso carbons *away* from the lobes of the d_{xy} orbital, thereby decreasing the already small overlap even further.

In contrast, the Fe–N$_P$ distance of ~1.95 Å would be a much more plausible site for significant orbital overlap, if the symmetry were correct. We note, in fact, that the pyrrole rings are twisted ~15° out of planarity with the mean plane of the porphyrin ring by the strong S_4 ruffling of the molecule (see Figure 2 and earlier discussion). This twisting creates a ~15° tilt in the orientation of the p$_z$ orbital of each porphyrin nitrogen in such a manner as to produce a (small) ($\pm$sin 15°) projection of the nitrogen p$_z$ orbital in the xy plane of the metal porphyrinate as a fraction of p$_x$ or p$_y$, as shown in Figure 10. Although the electron density (p$_x$ sin^2 15° or p$_y$ sin^2 15° $\approx$ 0.07p$_z$) is small, the favorable p$_x$ or p$_y$(N)–d$_{xy}$ orbital overlap should make this contribution considerably more significant than the p$_z$(C$_m$)–d$_{xy}$ overlap mentioned

(54) Pfaltz, A.; Jaun, B.; Fässler, A.; Eschenmoser, A.; Jaenchen, R.; Gilles, H. H.; Diekert, G.; Thauer, R. K. *Helv. Chim. Acta* **1982**, *65*, 828.

(55) Barkigia, K. M.; Thompson, M. A.; Fajer, J.; Pandey, R. K.; Smith, K. M.; Vincente, M. G. H. *New J. Chem.* **1992**, *16*, 599.

(56) Sparks, L. D.; Medforth, C. J.; Park, M.-S.; Chamberlain, J. R.; Ondrias, M. R.; Senge, M. O.; Smith, K. M.; Shelnutt, J. A. *J. Am. Chem. Soc.* **1993**, *115*, 581.

(57) Walker, F. A.; Simonis, U.; Zhang, H.; Walker, J. M.; Ruscitti, T. M.; Kipp, C.; Amputch, M. A.; Castillo, B. V.; Cody, S. H.; Wilson, D. L.; Graul, R. E.; Yong, G. J.; Tobin, K.; West, J. T.; Barichievich, B. A. *New J. Chem.* **1992**, *16*, 609.

(58) (a) Huet, J.; Gaudemer, A. *Org. Magn. Reson.* **1981**, *15*, 347. (b) Cassidei, L.; Bang, H.; Edwards, J. O.; Lawler, R. G. *J. Phys. Chem.* **1991**, *95*, 7186.

(59) Longuet-Higgins, H. C.; Rector, C. W.; Platt, J. R. *J. Chem. Phys.* **1950**, *18*, 1174.

7770   *J. Am. Chem. Soc., Vol. 116, No. 17, 1994*

Safo et al.
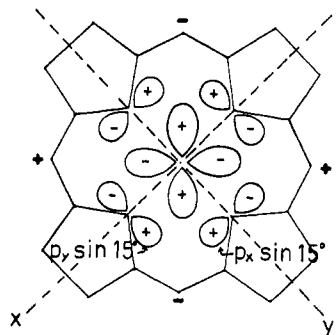
Figure 10. Possible interaction of the d_{xy} orbital with the porphyrin nitrogens in the case of strong S_4 ruffling. The remaining nitrogen p_x projections have proper symmetry to allow delocalization *via* the $a_{2u}(\pi)$ porphyrin orbital.

above. It also creates a remaining p_x orbital projection (p_z cos 15°) *and symmetry* that are consistent with the near-valence $a_{2u}(\pi)$ orbital of the porphyrin ring and not the $3e(\pi)$ set.[30,59] Thus, by ruffling the porphyrin core, the complex is able to stabilize the $(d_{xz}, d_{yz})^4 (d_{xy})^1$ electronic ground state *and* allow delocalization of the unpaired electron into the $a_{2u}(\pi)$ orbital of the porphyrin. In support of this means of spin delocalization from d_{xy} to the porphyrin ring by means of the four porphyrin nitrogens, it should be noted that the EPR spectra of metalloporphyrins having a d^1 ($= (d_{xy})^1$) electron configuration and metal isotopes with $I = 0$ ($Cr(V)$,[60,61] $Mo(V)$[62]) exhibit small superhyperfine splittings (a_N) from the porphyrin nitrogens, indicating electron spin delocalization from the d_{xy} orbital of the unpaired electron to the nitrogen nuclei. The size of a_N observed in these complexes (2.3–2.7 G)[60–62] is only 14–17% of that observed in the case of $CuTPP$,[63] where $d_{x^2-y^2}$ (which can overlap in a σ fashion with the porphyrin nitrogens) is the orbital of the unpaired electron. However, these and the isoelectronic vanadyl porphyrinates[64] are planar,[64d,e] nearly planar,[64a,e] or saddle-shaped[61] in the crystalline state, because

there are no axial ligand constraints to force them to ruffle. (Saddle-shaped porphyrinates would not have the proper N_P orbital symmetry for overlap with the d_{xy} orbital of the metal; however, in solution, where EPR spectra have been measured, they may be able to undergo deformations that include the type of S_4 ruffling observed for $[Fe(TPP)(4\text{-}CNPy)_2]ClO_4$ and its TMP analogs.) It is reasonable to expect that if the porphyrinate core were forced to ruffle, the size of the superhyperfine splittings could be much larger. Unfortunately, the EPR spectrum of the possible low-spin d^5 electron configurations is not sharp enough to observe ^{14}N superhyperfine splittings; however, pulsed EPR investigations of these systems, which may provide comparative information concerning the sizes of ^{14}N superhyperfine coupling constants for the two electronic ground states, are currently in progress in our laboratories.

Supplementary Material Available: Table SI, complete crystal data and intensity collection parameters for $[Fe(TPP)(4\text{-}CNPy)_2]$-$ClO_4$; Table SII, fractional atomic coordinates; Tables SIII and SIV, anisotropic thermal parameters and fixed hydrogen atom positions; and Table SVI, parameters added to the standard Macromodel MM2* parameter set (11 pages); Table SV, structure factor tables for $[Fe(TPP)(4\text{-}CNPy)_2]ClO_4$ (23 pages). This material is contained in many libraries on microfiche, immediately follows this article in the microfilm version of the journal, and can be ordered from the ACS; see any current masthead page for ordering information. Quick Time movies showing the porphyrin ring deformation are available through the ACS Gopher and anonymous FTP on the ACS server acsinfo.acs.org. Minimum computer hardware requirements for playing these movies are given in ref 46.

(60) Buchler, J. W.; Dreher, C.; Lay, K.-L.; Raap, A.; Gersonde, K. *Inorg. Chem.* **1983**, *22*, 879.

(61) Groves, J. T.; Takahashi, T.; Butler, W. M. *Inorg. Chem.* **1983**, *22*, 884.

(62) (a) Matsuda, Y.; Kubota, K.; Murakami, Y. *Chem. Lett. (Jpn.)* **1977**, 1281. (b) Bains, M. S.; Davis, D. G. *Inorg. Chim. Acta* **1979**, *37*, 53.

(63) Bohandy, J.; Kim, B. F. *J. Magn. Reson.* **1977**, *26*, 341.

(64) (a) Petersen, R. C. *Acta Crystallogr., Sect. B* **1969**, *25*, 2527. (b) Molinaro, F. S.; Ibers, J. A. *Inorg. Chem.* **1976**, *15*, 2278. (c) Ekstrom, A.; Fookes, C. J. R.; Hambley, T.; Loeh, H. J.; Miller, S. A.; Taylor, J. C. *Nature* **1983**, *306*, 173. (d) Miller, S. A.; Hambley, T. W.; Taylor, J. C. *Aust. J. Chem.* **1984**, *37*, 761. (e) Drew, M. G. B.; Mitchell, P. C. H.; Scott, C. E. *Inorg. Chim. Acta* **1984**, *82*, 63.